

Optical Fiber Breaks Due to Buckling: Problems in Device Packaging

NAOKI MITSUGI, HIROTOSHI NAGATA, MASARU SHIROISHI, NOBUHIDE MIYAMOTO, AND RYOSUKE KAIZU

Central Research Laboratories, Sumitomo Osaka Cement Co., Ltd., Toyotomi-cho 585, Funabashi-shi, Chiba 274, Japan

Received October 25, 1994

In order to achieve the hermetic sealing of optical device packages, the optical fibers are metalized and soldered to the package feed-throughs. Usually, reinforced metalized fibers are reliable, but it is found here that if a sufficiently large force is applied, the buckling of the metalized fiber end produces a break in the fiber at a force magnitude significantly lower than that required for nonmetalized fiber ends. Such breaks in the fiber could be the result of fibers protruding from their jacket ends due to shrinkage of the jacket materials. In order to avoid this problem and achieve more reliable packaging, the fibers must be designed to prevent deformation on both sides of the soldered points. © 1995 Academic Press, Inc.

1. INTRODUCTION

Hermetic sealing of optical fiber feed-throughs is required to achieve high reliability of optical devices for communication systems. In such devices, the fiber jackets are removed and the fiber surface is metalized to facilitate soldering to the package materials. For undersea devices, many sealing techniques where the metalized fibers and tension members are bounded together with the solder into the feed-through pipes have been proposed [1-4]. Yamazaki *et al.* reported a reliable design for the undersea repeater, which is based on a copper and gold metalization technique of the fibers coated with a very thin polyimide layer [5, 6]. The undersea high isotropic pressures and almost isothermal conditions are advantageous to maintaining the structural stability of packages, assuming that the moisture penetration problems are successfully solved. In contrast, the land-use devices are subject to heat cycles which can result in deformation of fibers and consequent breaks in fibers. Further, the strength of the exposed fibers decreases below the minimum for mechanical reliability of these devices, e.g., below the fiber-pull test criterion of > 1 kgf [7, 8]. Tensile strength of fibers soldered to feed-throughs was measured to be in the range of 0.5 to 1.5 kgf, suggesting that the fiber jackets themselves should be bonded to the package for additional mechanical reinforcement. In such a configuration, however, the fibers break if they are deformed between the soldered point and the other point fixed by adhesive material [7]. For instance, due to the thermal

shrinkage of the fiber jacket bonded at the package, the fibers could stick out from the jacket end and be buckled between the two fixed points [9]. In the conventional nylon tightjacketed fibers, the length by which the fibers stick out during heat cycle tests between -20 and 70°C was measured to be from less than a millimeter to a millimeter. This problem is remedied by the use of other jacketing materials such as polyester, polyvinyl chloride (PVC), and acrylate. The use of strong adhesive materials for the fiber jacket bonding is another possible solution [10].

The purpose of this report is to confirm experimentally the fiber breaks induced by the small buckling of the fibers which might occur in poorly designed packages. The results show that the fibers could be broken by a small buckling deformation such as that induced by the fiber protruding out from the nylon jacket. Further, the metal coat layer on the fiber was found to decrease the apparent strength of the fiber against the buckling. As a result, it is confirmed that designs which resist the fiber deformation are important in achieving a highly reliable fiber feed-through.

2. EXPERIMENTAL PROCEDURES

Figure 1 shows a schematic illustration of the equipment used in the present experiments. The fiber specimen was held straight between two brass sleeves without tensile stress. The bonding of the fiber and sleeve was done with a commercial adhesive material. The placement of the fiber in the sleeves was carried out with care to keep the fiber intact. One of the sleeves was fixed to the stage, and the other was connected to the plunger head of the micrometer. The fiber, held straight between the sleeves, was pushed slowly along the fiber axis until a buckling occurred. The push length which produced the break in the fiber was then read from the micrometer to an accuracy of 0.01 mm. In these experiments, the initial length of the fiber between the sleeves was set to be 5 mm, which resulted in a simple buckling deformation. When the longer fiber was set and pushed, it was deformed like a spiral and did not break.

The following six kinds of fiber samples, including fibers made by two Japanese manufacturers F and S, were evaluated.

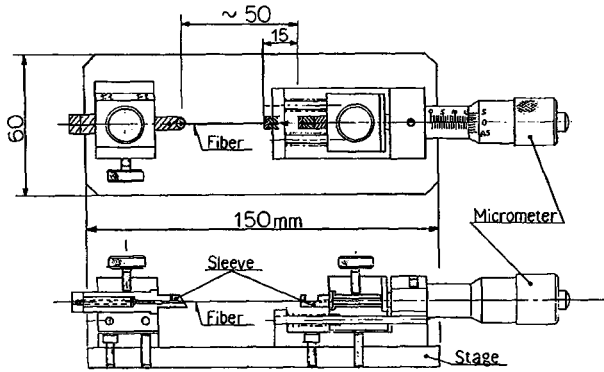


FIG. 1. Schematic illustration of the equipment to measure the critical push length for fiber breaks due to buckling deformation. The fiber is fixed to prevent bending between two sleeves, while the sleeve on the right side is pushed via a micrometer head. The break of the fiber is visually detected.

- (1) F' s single mode fibers (SMFs) with silicone primary coating layers.
- (2) F' s SMFs without silicone primary coating layers.
- (3) F' s polarization maintaining fibers (PMFs) without silicone primary coating layers.
- (4) S' s PMFs Without silicone primary coating layers.
- (5) S' s PMFs directly covered with Au/Ni plating layers.
- (6) No. (5) fibers with their Au/Ni plating layers removed by chemical etching.

In samples (2)–(6), the primary coating layers were removed using concentrated H_2SO_4 so as not to introduce flaws on the fiber surfaces after the outer nylon jackets had been mechanically removed [11, 12]. The Au/Ni layers of samples (5) and (6) were formed directly on the glass surface, just after the primary-coat removal, by a conventional electroless plating method. Thicknesses of the inner Ni and outer Au layers were 1–2 and 0.1–0.3 μm , respectively.

Figure 2 shows the Weibull plots of the results for sample (2), i.e., F' s SMFs Without resin coatings. The term X in the horizontal axis denotes the push length at which the fiber was broken, while $F(X)$ in the vertical axis denotes the cumulative fiber break probability at X . The distribution of the fiber breaks could be noticed in at least two regions. The first broad distribution below $X \sim 0.9$ mm ($\ln X \sim -0.11$) consisted of the fibers, all of which were broken at the point where the fiber was grasped by the brass sleeve. From the observation of fractofaces, the origins of such breaks could be attributed to surface flaws induced during the fiber pre-treatments and test processes. The fibers denoted by the other regions broke almost midway between the two sleeves, indicating these fibers were broken due to excess buckling deformation. All the experimental results hereinafter described included only the latter type of fiber breaks, and the data from the fibers which broke at the sleeve-end point were excluded.

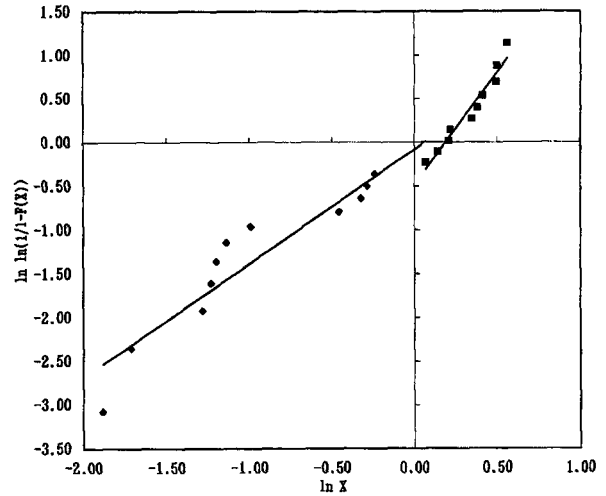


FIG. 2. Weibull plots for F' s SMF samples without silicone primary coating layers. The horizontal axis, $\ln X$, denotes natural logarithmic push length X (in mm) at the fiber break. The $F(X)$ denotes the cumulative break probability at X .

3. RESULTS AND DISCUSSION

3.1. Effects of the Primary Coatings

Figure 3 shows the Weibull plots of the results for F' s SMFs (1) with and (2) without the primary coating layers. The distribution of X values of the coated fibers (1) was narrow and $X = 1.3$ – 1.5 mm when the initial length was 5 mm. Their break points repeatedly occurred at the center region of the fiber. X values of the exposed fibers (2) covered a broader range between 0.9 and 1.7 mm. The fractofaces of both types of fibers were similar and split (see Fig. 4a), suggesting that

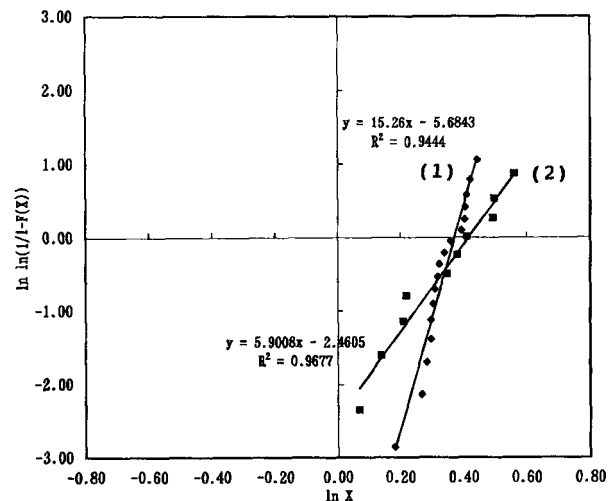


FIG. 3. Weibull plots for F' s SMF samples with (1) and without (2) silicone primary coating layers. The horizontal axis, $\ln X$, denotes natural logarithmic push length X (in mm) at the fiber break. The $F(X)$ denotes the cumulative break probability at X .

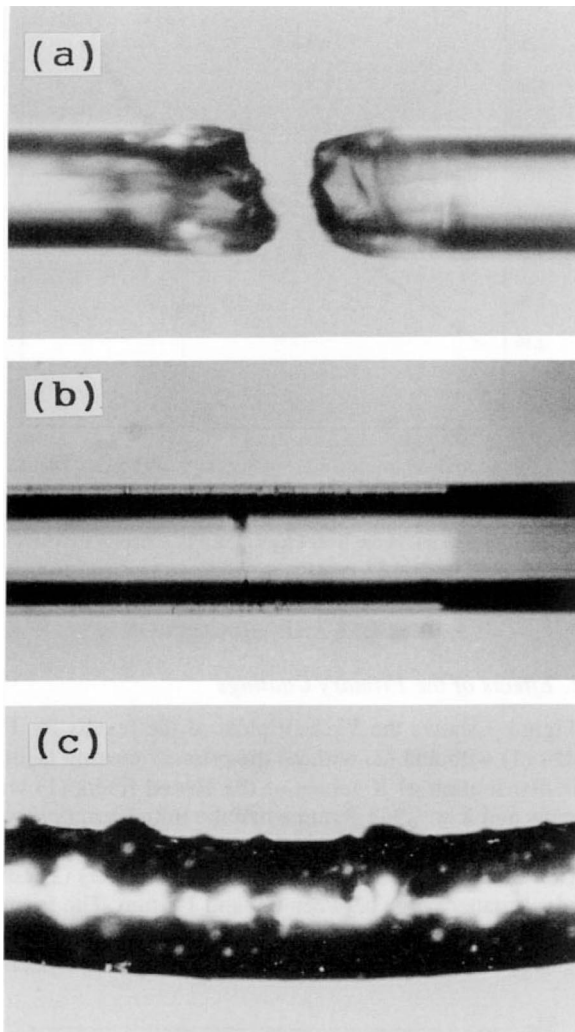


FIG. 4. Optical micrographs of the broken exposed SMF fiber (a) and the crack growth before the fiber break (b). (c) Shows the deterioration of the Au/Ni coating surface due to the fiber bending.

the fiber was intentionally broken at the region (not a point) where the bending stresses were concentrated. In the exposed fibers, it could be observed before breaking that many fine flaw marks grew normal to the fiber axis at the center point of the bent fiber (see Fig. 4b). The broader range of (2) might result from fractures originating in inevitable random microflaws of the exposed fiber surfaces. The characteristic X values, which correspond to $F(X) = 63.2\%$, were 1.45 mm for (1) and 1.52 mm for (2).

3.2. Results of PMF Samples

Because the PMF maintains the internal stresses mainly normal to its axis, a different fractophenomenon was expected between the PMF and SMF samples. In other bending tests of the PMF samples, for instance, some of the fractures were

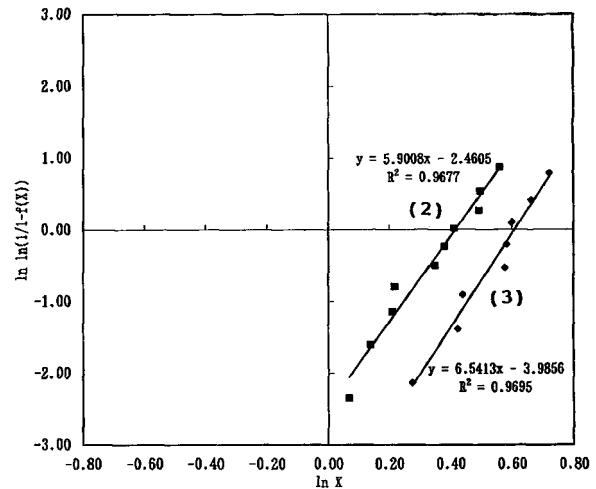


FIG. 5. Weibull plots for the exposed F' s SMF (2) and PMF (3) samples. The horizontal axis, $\ln X$, denotes natural logarithmic push length X (in mm) at the fiber break. The $F(X)$ denotes the cumulative break probability at X .

observed to proceed along the stress rods of the PMF. Figure 5 shows the Weibull plots where strengths of the exposed fibers of F' s SMF (2) and F' s PMF (3) are compared. The shapes of their data distributions, i.e., the gradients of their slopes, were almost the same, while the characteristic X value of the PMF (3) samples was 1.84 mm, larger than the 1.52 mm of the SMF (2). The introduction of the internal stresses to the fiber seemed to increase the resistance to the buckling, possibly because the directions of crack growth due to bending and surface stress induced by internal stress are mutually perpendicular. It is noted that the strengths of the SMFs and PMFs could be counted as similar in the package design.

3.3. Au/Ni Coated Fibers

Figure 6 exhibits the Weibull plots of the results for the exposed PMFs (4), Au/Ni-coated PMFs (5) and Au/Ni-coat-removed PMFs (6). These exposed PMFs from manufacturer S showed a similar data distribution and the characteristic X value of 1.58 mm as did those of F' s PMFs (2). The characteristic X values of the fibers (5) and (6) were 0.75 and 1.10 mm, respectively.

The Au/Ni-coated fibers broke unexpectedly under less strain than the uncoated fibers. As the fiber was bent, many flaw marks normal to the fiber appeared on the coating surface near the center of the fiber, and then the coating layer was partially lifted and peeled off (see Fig. 4c). The samples (6), in which the coating layer was chemically etched and removed, were stronger than the coated samples (5), suggesting that the Au/Ni plating treatment itself was not a dominant factor of fiber weakening. In regard to the low strengths of the Au/Ni-coated fibers, two possible reasons could be con-

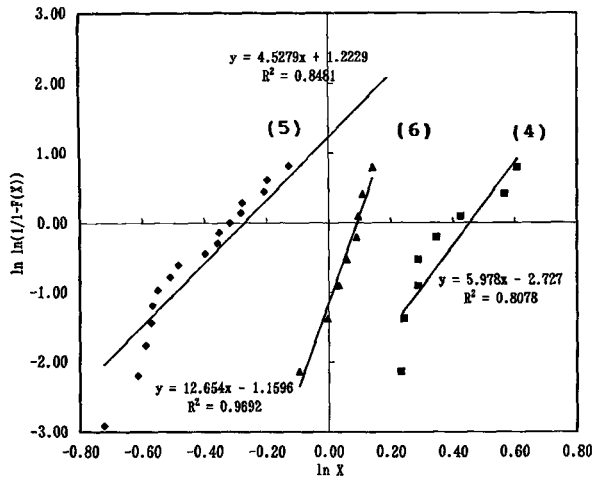


FIG. 6. Weibull plots for the exposed S' s PMF (4) and the Au/Ni-plated S' s PMF (5) samples. The sample (6) denotes the S' s PMF whose Au/Ni coatings are chemically removed before the test. The horizontal axis, $\ln X$, denotes natural logarithmic push length X (in mm) at the fiber break. The $F(X)$ denotes the cumulative break probability at X .

sidered. The first one is simple: the crack edges of the metal coated layer which grew due to fiber bending, injured the fiber surface; the other possibility is that the rough surface of the coating layer acted as a large fracture origin, as reported for the carbon coating of the fibers [13]. However, the second reason can be excluded here for the following considerations. After Griffith's law, the strength of the fiber is inversely proportional to the square root of the surface roughnesses [14, 15]. The surface roughnesses R_z measured with an atomic force microscope (AFM) were 2.01 nm for the exposed fiber and 182 nm for the Au/Ni-coated fiber. Therefore, it was predicted from Griffith's law that the strength of the coated fibers (5) was weaker than that of the exposed fibers (2) by a factor of 0.105. On the other hand, the stress induced in the outer surface of the bent fiber was inversely proportional to the separation distance D of the points fixing the fiber. Here, the D values for the fiber break were approximated by subtracting the characteristic value X from the initial fiber length of 5 mm and were calculated to be 3.42 and 4.25 mm for the exposed and Au/Ni-coated fiber samples, respectively. Consequently, from the present experimental results, the strength ratio of the fibers (5) to (2) was derived to be 0.805, significantly larger than the 0.105 calculated from Griffith's law, which suggests that the surface roughnesses of the Au/Ni coating did not dominantly influence the fiber strengths for the buckling deformation.

The strengths of the fibers, after their Au/Ni-plated layers were removed, were between those of the exposed and Au/Ni-plated fibers (see Fig. 6 (6)). A weakening in such fibers (6) rather than in the untreated fibers (4) could be attributed to the fact that surface roughnesses are possibly introduced

by chemical treatments in the plating process. Figure 7 shows the surfaces of the fibers before plating (a) and after etching the plating layers (b), corresponding to samples (4) and (6), respectively, observed by AFM. Their surface roughnesses R_z were 2.01 nm for (4) and 3.96 nm for (6). The strength ratio of (6) to (4) samples was estimated to be 0.713 from their surface roughnesses using Griffith's law and it was almost in agreement with the 0.877 derived from the characteristic D values in this experiment. Further, the narrow data distribution of the sample (6) suggested that the degree of surface erosion due to the plating process could be controlled.

4. PACKAGE DESIGN DESIRED FOR RELIABLE FIBER ASSEMBLY

From the above experimental results, it was concluded that fibers must be kept straight and hermetically packed especially when the assembled fibers length is short. The metal coating of the exposed fiber surface did not reinforce the fiber enough to prevent buckling deformation. Therefore, package designs which include fiber assembled to be intentionally bent or offset against the axis should be reexamined from the viewpoint of possible future fiber breaks, although such designs are suitable for avoiding other fiber breaks due to a

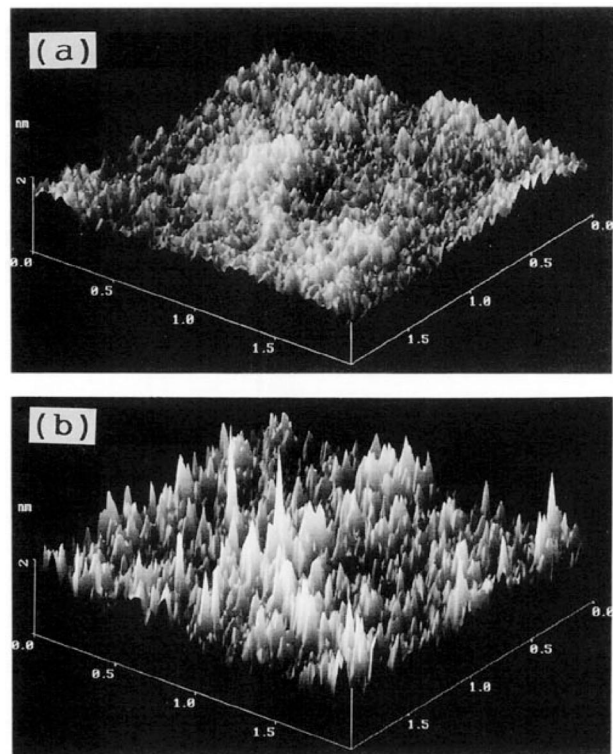


FIG. 7. Atomic force micrographs of the typical exposed fiber surface of the sample (4) (a) and the surface of sample (6) after removal of the Au/Ni layer (b). The scan area (x - y -plane) is $2 \times 2 \mu\text{m}^2$, and the height of the z -axis is 2 nm.

mismatch of thermal expansion of the fiber and package materials [16, 17]. Further, the undesirable fiber buckling should also be excluded by proper package design. Possible origins of buckling are thermal shrinkage of the fiber jacket materials and uncontrolled adhesive strengths between jacket layers. The fibers tightly jacketed with elastomer materials, such as polyester and PVC, are known to be significantly better in this regard than with the nylon tight-jacketed fibers. Use of such highly reliable fibers and additionally a tight structural design of the fiber feed-through to prevent bending the fiber should be important factors for the achievement of high reliability in fiber packaging technology.

ACKNOWLEDGMENTS

The authors are greatly indebted to Drs. T. Honda and J. Minowa for helpful discussions, Dr. E. Min for AFM observation of the fibers, and many collaborators of Optoelectronics Lab. of Sumitomo Osaka Cement Co., Ltd.

REFERENCES

- [1] K. Kobayashi, Y. Ejiri, A. Nagai, K. Sanada, and K. Mochizuki, "Joining of OS-280M optical fiber submarine cable," in *Proc. International Conf. on Optical Fiber Submarine Telecommunication System, SUBOPTIC '86*, Paris, France, pp. 253–258, paper Communication 9.1, 1986.
- [2] I. Kitazawa, H. Okamura, and S. Nakamura, "FS-400M submarine optical repeater housing," *J. Lightwave Technol.*, vol. LT-2, no. 6, 870 (1984).
- [3] S. Nishi and N. Takahara, "Optical-fiber feedthrough in pressure housing," *J. Lightwave Technol.*, vol. LT-2, no. 6, 883 (1984).
- [4] M. W. Perry, G. A. Reinold, and P. A. Yeisley, "Physical design of the SL repeater," *J. Lightwave Technol.*, vol. LT-2, no. 6, 863 (1984).
- [5] Y. Yamazaki, K. Furusawa, O. Harada, H. Nakashima, I. Sakurai, and M. Kondoh, "Fiber seal design for OS-280M optical fiber submarine repeater," in *Proc. International Conf. on Optical Fiber Submarine Telecommunication System, SUBOPTIC '86*, Paris, France, pp. 219–224, paper Communication 7.6, 1986.
- [6] Y. Yamazaki, Y. Ejiri, and K. Furusawa, "Design and test results of an optical fiber feedthrough for an optical submarine repeater," *J. Lightwave Technol.*, vol. LT-2, no. 6, 876 (1984).
- [7] B. G. LeFevre, W. W. King, A. G. Hardee, A. W. Carlisle, and K. B. Bradley, "Failure analysis of connector-terminated optical fibers: two case studies," *J. Lightwave Technol.*, vol. 11, no. 4, 537 (1993).
- [8] Technical Reference TR-NWT-000468, Issue 1, "Reliability assurance practices for optoelectronic devices in interoffice applications," Bellcore, Red Bank, NJ, 1991.
- [9] E. Suhir, "Interfacial shearing stress in pull-out testing of dual-coated lightwave specimens," *J. Lightwave Technol.*, vol. 11, no. 12, 1905 (1993).
- [10] M. Wada, "Adhesive materials for optical fiber assembly: Epo-Tek," *Optronics*, no. 3, 103 (1991) [in Japanese].
- [11] H. Nagata, N. Miyamoto, and R. Kaizu, "Highly reliable jacket cutter for optical fibers," *IEICE Trans. Fundamentals Electron. Commun. Comput. Sci.*, vol. E76-A, no. 7, 1263 (1993).
- [12] H. Nagata, N. Miyamoto, T. Saito, and R. Kaizu, "Reliable jacket stripping of optical fibers," *J. Lightwave Technol.*, vol. 12, no. 5, 727 (1994).
- [13] N. Yoshizawa, H. Tada, and Y. Katsuyama, "Strength improvement and fusion splicing for carbon-coated optical fiber" *J. Lightwave Technol.*, vol. 9, no. 4, 417 (1991).
- [14] R. S. Robinson and H. H. Yuce, "Scanning tunneling microscopy of optical fiber corrosion: surface roughness contribution to zero stress aging," *J. Am. Ceram. Soc.*, vol. 74, no. 4, 814 (1991).
- [15] V. V. Rondinella and M. J. Matthewson, "Coating additives for improved mechanical reliability of optical fiber," *J. Am. Ceram. Soc.*, vol. 77, no. 1, 73 (1994).
- [16] E. Suhir, C. Paola, and W. N. MacDonald, "Input/output fiber configuration in a laser packaging design," *J. Lightwave Technol.*, vol. 11, no. 12, 2087 (1991).
- [17] H. Jumonji and T. Nozawa, "Instabilities and their characterization in Mach-Zehnder Ti:LiNbO₃ optical modulator," *IEICE Trans.*, vol. J-75-C-1, 17 (1992) [in Japanese].